

Real-Time Observation of the Self-Assembly of Hybrid Polyoxometalates Using Mass Spectrometry**

Elizabeth F. Wilson, Haralampos N. Miras, Mali H. Rosnes, and Leroy Cronin*

Polyoxometalate (POM) clusters constitute a wide and varied family of structures formed by condensation reactions of metal oxide anions of early transition metals, for example, V, Mo, and W, in high oxidation states.^[1] Their size can vary from sub-nanoscale to protein-sized clusters,^[2] and their interesting electronic and molecular properties^[3] have led to many potential applications for POMs, in areas as diverse as catalysis,^[3,4] medicine,^[1] and materials science.^[5]

One of the most interesting aspects of POM chemistry lies with the fact that the clusters can be viewed as transferable building blocks or synthons,^[6a] the controlled assembly of which is desirable in order to synthesize novel architectures with functionality. However, despite the increasingly intensive research in this area, understanding of the complex formation mechanisms and self-assembly processes which govern POM structure formation remains limited.^[6] In practice, this lack of understanding leads to experimentation where manipulation of reaction parameters in the commonly used “one-pot” POM syntheses often leads to the formation of new POM structures, albeit by a somewhat serendipitous approach.^[2]

For example, in the area of organic-inorganic POM hybrid compounds, although solid-state investigations using tris(alkoxo) ligands with POMs have been carried out, that is, using Anderson,^[7,8] Lindqvist,^[9] and Dawson^[5a,10] structural types, along with investigations of other POM architectures,^[11–13] there has been very little research into the self-assembly processes which govern the formation of these structures in solution. In particular, the use of mass spectrometry (MS) to aid elucidation of the rearrangements and aggregation processes involved has, so far, been neglected. Thus, there is a clear and urgent need to develop approaches to bridge the gap^[14,15] between solid-state and solution studies so that the key features of the self-assembly mechanisms of polyoxometalate clusters can be revealed.

Herein, the use of electrospray ionization mass spectrometry (ESI-MS) has allowed real-time, “in-solution” monitoring of the formation of a complex, organic-inorganic POM hybrid system. The reaction system chosen for investigation was found by Hasenknopf and co-workers^[7b] and involves the rearrangement of $[\alpha\text{-Mo}_8\text{O}_{26}]^{4-}$, coordination of Mn^{III} , and coordination of two tris(hydroxymethyl)aminomethane molecules (TRIS), to form the symmetrical Mn-Anderson cluster $((n\text{-C}_4\text{H}_9)_4\text{N})_3[\text{MnMo}_6\text{O}_{18}((\text{OCH}_2)_3\text{CNH}_2)_2]$ (**1**; also written as $\text{TBA}_3[\text{MnMo}_6\text{O}_{18}((\text{OCH}_2)_3\text{CNH}_2)_2]$; Figure 1). This work builds upon our earlier studies of using mass spectrometry to

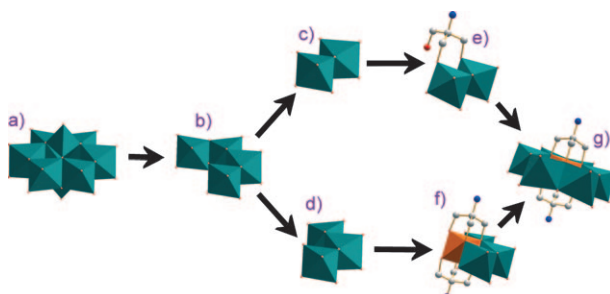


Figure 1. Illustration to visualize the prominent, intermediate fragment ions identified in this study (labeled b–f), which are involved in the rearrangement of the $[\alpha\text{-Mo}_8\text{O}_{26}]^{4-}$ anion (labeled a), into the symmetrical Mn-Anderson anion $[\text{MnMo}_6\text{O}_{18}((\text{OCH}_2)_3\text{CNH}_2)_2]^{3-}$ of **1** (labeled g).^[7b] Structures (b–f) (formal representations based on crystallographic data^[7b] are shown here) represent the following fragment ions identified in these ESI-MS investigations: b) $[\text{Mo}_4\text{O}_{13}\text{TBA}]^{-}$, c) $[\text{Mo}_2\text{O}_7\text{H}]^{-}$, d) $[\text{Mo}_3\text{O}_{10}\text{TBA}]^{-}$, e) $[\text{Mo}_2\text{O}_5((\text{OCH}_2)_3\text{CNH}_2)]^{-}$, f) $[\text{Mn}^{\text{III}}\text{Mo}_3\text{O}_8((\text{OCH}_2)_3\text{CNH}_2)]^{-}$. Color scheme: Mo green polyhedra, Mn orange polyhedra, O red, N blue, C gray spheres. H atoms are omitted for clarity.

investigate a simpler reaction system, wherein the formation of the silver-linked β -octamolybdate structure $((n\text{-C}_4\text{H}_9)_4\text{N})_{2n}[\text{Ag}_2\text{Mo}_8\text{O}_{26}]_n$ was investigated.^[16]

The reaction system forming POM hybrid **1** was selected for investigation for a number of reasons. First, it presents a conveniently accessible, complex cluster rearrangement forming an organic-inorganic POM hybrid structure. Also, as such organic-inorganic POM hybrids can be used as synthons in the design of nanoscale hybrid POM architectures, increasing our knowledge of the aggregation processes which form such building blocks will make the field of nanoscale functional materials more accessible for further exploration. Moreover, this reaction takes place in acetonitrile solution which is a volatile, moderately polar solvent suitable for use in MS investigations and which usually provides MS data of polyoxometalates with a good signal-to-noise ratio and

[*] Dr. E. F. Wilson,^[++] Dr. H. N. Miras,^[+] M. H. Rosnes, Prof. L. Cronin WestCHEM, Department of Chemistry, University of Glasgow Glasgow, G12 8QQ, Scotland (UK)
Fax: (+44) 141-330-4888
E-mail: l.cronin@chem.gla.ac.uk
Homepage: <http://www.croninlab.com>

[++] Current address: Department of Chemistry and Pharmacy Inorganic Chemistry, University of Erlangen-Nürnberg Egerlandstrasse 1, 91058 Erlangen (Germany)

[+] These authors contributed equally to this work.

[**] We acknowledge financial support from the EPSRC, the Royal Society of Edinburgh, and Marie Curie actions, and collaborative work with Bruker Daltonics Ltd.

Supporting information for this article is available on the WWW under <http://dx.doi.org/10.1002/anie.201006938>.

reliable transmission of ions which reflect their relative concentrations in solution.^[15–17]

The speciation and fragment rearrangements were investigated as follows. Tetrabutylammonium α -octamolybdate, $((n\text{-C}_4\text{H}_9)_4\text{N})_4[\alpha\text{-Mo}_8\text{O}_{26}]$, manganese(III) acetate, and TRIS were suspended in acetonitrile solution and stirred at room temperature for approximately 15 minutes, before heating at reflux at 80°C for approximately 30 h. Aliquots were removed at noted time intervals throughout the reaction, diluted with acetonitrile, and analyzed using ESI-MS (the parameters for which were consistent throughout all runs). The first spectrum was recorded after the reaction solution had been stirred at room temperature for 13 minutes. This spectrum is dominated by peaks which can be assigned to isopolyoxomolybdate fragments of the rearranging $[\alpha\text{-Mo}_8\text{O}_{26}]^{4-}$ anion (Figure 2 and Table S2 in the Supporting Information) and contains the ion series:

- 1) $[\text{H}_{m-2}\text{Mo}_m\text{O}_{3m}]^-$ where $m=2$ or 3
- 2) $[\text{Mo}_m\text{O}_{3m+1}]^{2-}$ where $m=4$ or 5
- 3) $[\text{Na}_n\text{H}_{1-n}\text{Mo}_m\text{O}_{3m+1}]^-$ where $m=3$ or 4 and $n=0$ or 1
- 4) $[\text{H}_2\text{Mn}^{\text{II}}\text{Mo}_m\text{O}_{3m+1}]^-$ where $m=3$ or 4
- 5) $[\text{Mo}_m\text{O}_{3m+1}\text{TBA}_1]^-$ where $m=3$ –5
- 6) $[\text{Mo}_8\text{O}_{26}\text{TBA}_{3-n}\text{Na}_n]^-$ where $n=0$ –2

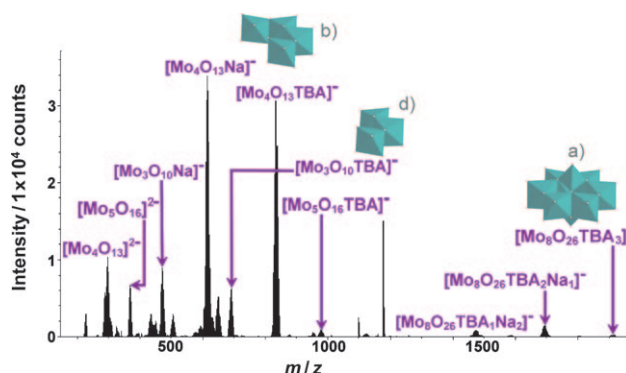


Figure 2. ESI mass spectrum collected from the reaction solution of **1**, recorded after it had been stirred at room temperature for 13 minutes. The spectrum is dominated by isopolyoxomolybdate fragment peaks. Of particular note is that the two major peaks in this spectrum, at m/z 614.6 (the base peak) and 833.8, are attributed to the species $[\text{Mo}_4\text{O}_{13}\text{Na}]^-$ and $[\text{Mo}_4\text{O}_{13}\text{TBA}]^-$, respectively, that is, half of the parent $(\text{Mo}_8\text{O}_{26})^{4-}$ cluster anion. Some of the intermediate, prominent fragment ions shown in Figure 1 (formal representations based on crystallographic data^[7b]) are also shown here and are labeled similarly. Color scheme as in Figure 1.

The dominance of these isopolyoxomolybdate fragments indicates that the $[\alpha\text{-Mo}_8\text{O}_{26}]^{4-}$ anion rearranges into these smaller fragment ions prior to further coordination with the Mn cations and TRIS groups. Indeed the first indications of this further coordination are illustrated by the presence of very low intensity peaks corresponding to fragments containing TRIS groups and manganese cations, for example, $[\text{Mo}_2\text{O}_5((\text{OCH}_2)_3\text{CNH}_2)]^-$ (m/z 387.8), and $[\text{Mn}^{\text{III}}\text{Mo}_3\text{O}_8((\text{OCH}_2)_3\text{CNH}_2)_2]^-$ (m/z 706.7; Table S2 in the Supporting Information).

The spectrum recorded after the reaction mixture had been heated at reflux for approximately 7 h (Figure S1 in the Supporting Information) can be seen to have increased in complexity. The dominant peaks are now assigned to a wide variety of fragments: polyoxomolybdate fragments coordinated to Mn cations, for example, $[\text{Mn}^{\text{II}}\text{Mo}^{\text{VI}}\text{Mo}^{\text{V}}\text{O}_7]^-$ (peak at m/z 358.7); polyoxomolybdate fragments coordinated to TRIS, for example, $[\text{Mo}_2\text{O}_5((\text{OCH}_2)_3\text{CNH}_2)]^-$ (peak at m/z 389.8); and fragments of the product cluster **1**, for example, $[\text{Mn}^{\text{III}}\text{Mo}_3\text{O}_8((\text{OCH}_2)_3\text{CNH}_2)_2]^-$ (peak at m/z 706.7).

The ion series identified at this point in the reaction are:

- 1) $[\text{H}_{m-2}\text{Mo}_m\text{O}_{3m}]^-$ where $m=2$ or 3
- 2) $[\text{HMo}_m\text{O}_{3m+1}]^-$ where $m=2$ or 3
- 3) $[\text{HMn}^{\text{II}}\text{Mo}_m\text{O}_{3m+2}]^-$ where $m=2$ or 3
- 4) $[\text{Mo}_m\text{O}_{3m-1}((\text{OCH}_2)_3\text{CNH}_2)]^-$ where $m=2$ or 3
- 5) $[\text{Mn}^{(n+2)+}\text{Mo}_3\text{O}_{9+n}((\text{OCH}_2)_3\text{CNH}_2)\text{H}]^-$ where $n=0$ or 1
- 6) $[\text{Mn}^{\text{III}}\text{Mo}_m\text{O}_{3m-1}((\text{OCH}_2)_3\text{CNH}_2)_2]^-$ where $m=2$ –5
- 7) $[\text{Mn}^{\text{III}}\text{Mo}_6\text{O}_{18}((\text{OCH}_2)_3\text{CNH}_2)_2\text{TBA}_{2-n}\text{H}_n]^-$ where $n=0$ or 1
- 8) $[\text{Mo}_m\text{O}_{3m+1}\text{TBA}_1]^-$ where $m=3$ or 4

The complexity and ion series observed in this spectrum remains observable through to the final spectrum recorded after the reaction mixture had been heated at reflux for approximately 30 h (see Figures 3 and 4 and Table S3 in the

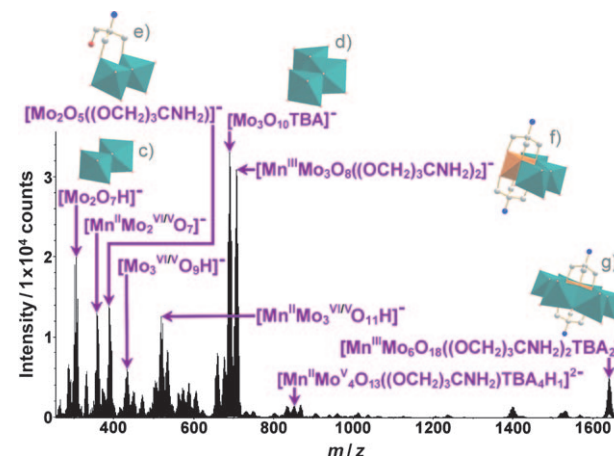


Figure 3. ESI mass spectrum collected from the reaction solution of **1**, recorded after it had been heated at reflux (80°C) for approximately 30 h. Some of the intermediate, prominent fragment ions shown in Figure 1 (formal representations based on crystallographic data^[7b]) are also shown here and are labeled similarly. Color scheme as in Figure 1.

Supporting Information). It is interesting to note at this point the presence of Mn^{II} ions, particularly in the smaller m/z fragment ions, and mixed-oxidation-state species where molybdenum is found to exist in oxidation states IV, V, and VI. Observation of molybdenum and manganese centers in reduced oxidation states is not entirely unexpected as they are a consequence of the high voltages utilized in the mass spectrometry ion-transfer process.^[18] Also the singly reduced molybdate species $[\text{Mo}^{\text{V}}\text{O}_3]^-$ and the corresponding singly reduced tungstate species $[\text{W}^{\text{V}}\text{O}_6]^-$ have been observed in

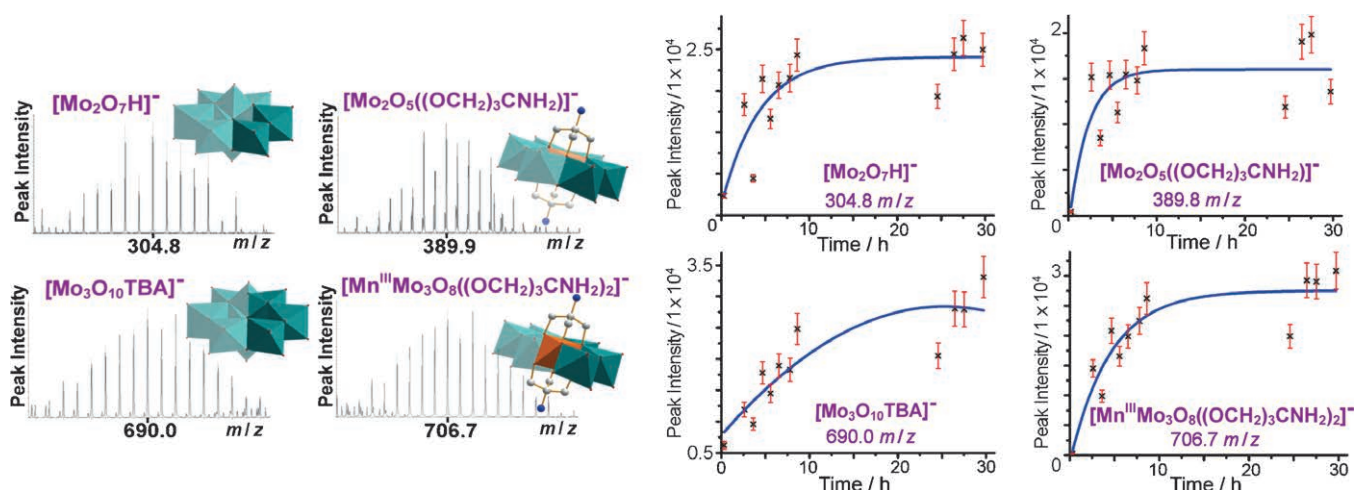


Figure 4. Left: Experimental mass spectra of some prominent small fragment ions observed during ESI-MS monitoring of the reaction solution of **1**. The structures shown (formal representations based on crystallographic data^[7b]) are useful to indicate the role of these fragments as building blocks of the “parent” octamolybdate and Mn-Anderson-TRIS clusters. Color scheme as in Figure 1. H atoms are omitted for clarity. Right: Graphs showing the general trends of increasing peak intensity of these prominent small fragment ions over time, observed during ESI-MS monitoring of reaction solution of **1** over approximately 30 h. Lines of best fit are shown as a guide for the eye only. Intensity in number of counts.

previous studies,^[19] along with mixed-oxidation-state fragments of polyoxomolybdate ions.^[20a,16] Mixed-oxidation-state fragments of polyoxochromate systems have also been identified in solutions previously during the course of ESI-MS studies.^[20b]

Of paramount importance herein is that further information, about the rearrangement processes taking place in solution from $[\alpha\text{-Mo}_8\text{O}_{26}]^{4-}$ to the formation of the product cluster anion $[\text{MnMo}_6\text{O}_{18}((\text{OCH}_2)_3\text{CNH}_2)_2]^{3-}$, can be reliably extracted from the ESI-MS data by monitoring the reaction as a function of time. This is because, by plotting the intensities of the peaks assigned against the time of MS sampling, we can build up a qualitative picture of how the concentration of various species in solution varies over the time of reaction. This approach was used successfully in our earlier investigations into the rearrangements of the molybdenum-Lindqvist cluster $[\text{Mo}_6\text{O}_{19}]^{2-}$ in the presence of silver(II) cations, into the silver-linked β -octamolybdate structure $((n\text{-C}_4\text{H}_9)_4\text{N})_{2n}[\text{Ag}_2\text{Mo}_8\text{O}_{26}]_n$,^[16] and also in our work on Dawson-based clusters.^[21] The Dawson-based work is important since it demonstrates the possibility to directly correlate the concentration of the transmitted intermediate and product ion species in the gas phase with the parent species in solution.^[21] Similarly here, it is important to note that the intensity growth of the product-related peaks and the intensity decrease of the reactant-related species are correlated, and we were able to prove that some intermediates are “intrinsic” to the reaction mechanism as a result of in situ collision studies.

Therefore, through the use of this qualitative approach it can be observed that both the intensity of the $[\text{Mo}_8\text{O}_{26}\text{TBA}_3]^-$ peak (at m/z 1911.0) and the $[\text{Mo}_4\text{O}_{13}\text{TBA}]^-$ peak (at m/z 833.8) decrease exponentially (i.e. within approximately 1.5 h) to minimum, constant values (Figures S2 and S3 in the Supporting Information), whilst the intensity of the

product anion $[\text{Mn}^{III}\text{Mo}_6\text{O}_{18}((\text{OCH}_2)_3\text{CNH}_2)_2\text{TBA}_2]^-$ peak (at m/z 1640.0) increases at a lower respective rate over the course of the reaction (Figure S5 in the Supporting Information). The decrease in reactant ion peak intensity and the subsequent increase in product ion peak intensity is not surprising; however, the difference in speed of decomposition of the $[\text{Mo}_8\text{O}_{26}\text{TBA}_3]^-$ ion and formation of the product $[\text{Mn}^{III}\text{Mo}_6\text{O}_{18}((\text{OCH}_2)_3\text{CNH}_2)_2\text{TBA}_2]^-$ ion suggests the mechanism of formation proceeds through further intermediate, rate-determining steps which then govern the rate of final product ion formation. It is interesting to note the changes in intensity of the peaks assigned to the small fragment ions $[\text{Mo}_2\text{O}_7\text{H}]^-$ (m/z 304.8), $[\text{Mo}_2\text{O}_5((\text{OCH}_2)_3\text{CNH}_2)]^-$ (m/z 389.8), $[\text{Mo}_3\text{O}_{10}\text{TBA}]^-$ (m/z 690.0), and $[\text{Mn}^{III}\text{Mo}_3\text{O}_8((\text{OCH}_2)_3\text{CNH}_2)_2]^-$ (m/z 706.7) over the course of the reaction. These peaks are prominent throughout all the spectra taken after a reaction time of 1 h 20 min, and their intensities, and hence concentrations, are all observed to increase over reaction time (Figure 4).

These observations, when considered as a whole, are extremely important in increasing our understanding of the rearrangement processes taking place in the reaction solution. First, the exponential decrease in peak intensity of the $[\text{Mo}_8\text{O}_{26}\text{TBA}_3]^-$ and the $[\text{Mo}_4\text{O}_{13}\text{TBA}]^-$ ions could suggest an initial, rapid decomposition and rearrangement of $[\alpha\text{-Mo}_8\text{O}_{26}]^{4-}$ ions through the formation of the $[\text{Mo}_4\text{O}_{13}]^{2-}$ cluster species; in other words, $[\text{Mo}_4\text{O}_{13}\text{Na}_1]^-$ (m/z 614.6, base peak) and $[\text{Mo}_4\text{O}_{13}\text{TBA}]^-$ (m/z 833.8), which are half-fragments of the $\{\alpha\text{-Mo}_8\}$ clusters and the most prominent peaks in the first spectrum recorded (see Figure 2), rearrange into the smaller, stable dinuclear, $[\text{Mo}_2\text{O}_7\text{H}]^-$, and trinuclear, $[\text{Mo}_3\text{O}_{10}\text{TBA}]^-$, isopolyoxomolybdate fragments. The concomitant increase in peak intensity of these small isopolyoxomolybdate ions over the time of reaction supports this proposal. Then the identification of similar dinuclear and

trinuclear molybdate fragments possessing further coordination with TRIS and manganese ions— $[\text{Mo}_2\text{O}_5((\text{OCH}_2)_3\text{CNH}_2)]^-$ and $[\text{Mn}^{\text{III}}\text{Mo}_3\text{O}_8((\text{OCH}_2)_3\text{CNH}_2)_2]^-$ —and their concentrations which also increase over the time of reaction, suggest subsequent coordination of these building blocks with TRIS, manganese ions, and further molybdate anionic units, hence building-up the final Mn-Anderson-TRIS product ion. An illustration of these decomposition, then product self-assembly steps, involving these small, intermediary fragment ions is shown in Figure 1.

It is also important to note here that the peak assignments of these small fragment ions, as well as the suggestion that they could act as intermediates in the formation of the full Mn-Anderson-TRIS cluster, are further supported by previous solid-state studies in which rearrangement of $[\alpha\text{-Mo}_8\text{O}_{26}]^{4-}$ clusters into small, stable fragment ions such as $[\text{Mo}_2\text{O}_7\text{H}]^-$ has been investigated,^[6b,22] and similar bi- and tri(oxomolybdate) anions coordinated to tris(alkoxo) ligands have been isolated and characterized using single-crystal X-ray diffraction.^[12]

Another noticeable feature of the MS data of this reaction system is the increasing prominence of the peaks attributed to $[\text{Mo}_3\text{O}_{10}\text{TBA}]^-$ (m/z 690.0) and $[\text{Mn}^{\text{III}}\text{Mo}_3\text{O}_8((\text{OCH}_2)_3\text{CNH}_2)_2]^-$ (m/z 706.7) as the reaction proceeds. Indeed in the final spectrum, recorded after approximately 30 h of heating at reflux, the $[\text{Mo}_3\text{O}_{10}\text{TBA}]^-$ (m/z 690.0) peak is the base peak, with the $[\text{Mn}^{\text{III}}\text{Mo}_3\text{O}_8((\text{OCH}_2)_3\text{CNH}_2)_2]^-$ (m/z 706.7) peak at only slightly lower intensity (see Figure 3).

In an effort to confirm that the aforementioned species are intermediate products of the reaction mechanism and not products of the final product's fragmentation during the course of the MS studies, we isolated $[\text{Mn}^{\text{III}}\text{Mo}_3\text{O}_8((\text{OCH}_2)_3\text{CNH}_2)_2]^-$ (peak at m/z 706.7) and $[\text{Mn}^{\text{III}}\text{Mo}_6\text{O}_{18}((\text{OCH}_2)_3\text{CNH}_2)_2\text{TBA}_2]^-$ (peak at m/z 1640.0) by trapping the species and we studied their behavior individually as a function of the applied collision energy. As we expected, the final product $[\text{Mn}^{\text{III}}\text{Mo}_6\text{O}_{18}((\text{OCH}_2)_3\text{CNH}_2)_2\text{TBA}_2]^-$ (peak at m/z 1640.0) fragmented only after considerable increase of the collision energy at a value of 30 eV (Figure S6 in the Supporting Information). Furthermore, using a similar approach in the case of $[\text{Mn}^{\text{III}}\text{Mo}_3\text{O}_8((\text{OCH}_2)_3\text{CNH}_2)_2]^-$ (m/z 706.7) proved that the species retained their integrity at the collision energies (10 eV) we used during the course of the actual studies. Additionally the species fragmented only when the collision energy reached a value of 20 eV (Figure S7 in the Supporting Information). All the above-mentioned data indicate that the species $[\text{Mo}_3\text{O}_{10}\text{TBA}]^-$ (m/z 690.0) and $[\text{Mn}^{\text{III}}\text{Mo}_3\text{O}_8((\text{OCH}_2)_3\text{CNH}_2)_2]^-$ (m/z 706.7) which exist in the final reaction mixture are equilibrium intermediates and consequently part of the formation mechanism and not fragmentation products. An explanation for this, as suggested in a study by Zubietta and Khan^[12c] as well as by Müller et al.,^[13] is that correlation of the tripodal geometry of the TRIS ligand with the $[\text{Mo}_3]$ anionic units, and the ability of the organic ligand to reduce the charge density of this building block unit, both act to lend greater stability to these trimolybdate-centered equilibrium species.

In summary, we have for the first time utilized the technique of ESI-MS to monitor the real-time, “in-solution” formation of a complex organic-inorganic POM hybrid system. The system chosen for study involved the rearrangement of $[\alpha\text{-Mo}_8\text{O}_{26}]^{4-}$, coordination of Mn^{III} , and coordination of two TRIS molecules to form the symmetrical Mn-Anderson cluster $((n\text{-C}_4\text{H}_9)_4\text{N})_3[\text{MnMo}_6\text{O}_{18}((\text{OCH}_2)_3\text{CNH}_2)_2]$ (**1**). Through assignment of the fragment ions observed in the ESI mass spectra of the reaction solution of **1**, and by noting the changes in peak intensity of prominent peaks in these spectra over the time of reaction, we have been able to propose that the rearrangement of $[\alpha\text{-Mo}_8\text{O}_{26}]^{4-}$ occurs first through the formation of $[\text{Mo}_4\text{O}_{13}]^{2-}$ cluster species (i.e. $[\text{Mo}_4\text{O}_{13}\text{Na}_1]^-$ (m/z 614.6) and $[\text{Mo}_4\text{O}_{13}\text{TBA}]^-$ (m/z 833.8)) which are half-fragments of the $\{\text{Mo}_8\}$ clusters and the most prominent peaks in the first spectrum recorded (see Figure 2). We propose this is then followed by decomposition to smaller, stable isopolyoxomolybdate fragment ions containing just two ($[\text{Mo}_2\text{O}_7\text{H}]^-$) and three molybdenum centers ($[\text{Mo}_3\text{O}_{10}\text{TBA}]^-$), which subsequently coordinate with the tripodal TRIS ligands, ($[\text{Mo}_2\text{O}_5((\text{OCH}_2)_3\text{CNH}_2)]^-$ (m/z 389.8)), manganese ions ($[\text{Mn}^{\text{III}}\text{Mo}_3\text{O}_8((\text{OCH}_2)_3\text{CNH}_2)_2]^-$ (m/z 706.7)), and further molybdate anionic units, to form the final Mn-Anderson-TRIS cluster $[\text{Mn}^{\text{III}}\text{Mo}_6\text{O}_{18}((\text{OCH}_2)_3\text{CNH}_2)_2\text{TBA}_2]^-$ (**1**; m/z 1640.0). Additionally, fragmentation studies of the $[\text{Mn}^{\text{III}}\text{Mo}_3\text{O}_8((\text{OCH}_2)_3\text{CNH}_2)_2]^-$ (m/z 706.7) and $[\text{Mn}^{\text{III}}\text{Mo}_6\text{O}_{18}((\text{OCH}_2)_3\text{CNH}_2)_2\text{TBA}_2]^-$ (peak at m/z 1640.0) demonstrated the resilience of the aforementioned species during the course of the actual MS studies while at the same time confirmed that the trimolybdate-centered species at m/z 690.0 and 706.7 are equilibrium-stable intermediates of the Mn-Anderson formation mechanism.

In future work we will use real-time mass spectrometry to study more complex cluster systems, apply this technique to a wide range of nanomolecular systems to examine the self-assembly processes governing the formation of the structures, and develop more robust analytical standards that allow quantitative analysis.

Experimental Section

The reaction solution of $((n\text{-C}_4\text{H}_9)_4\text{N})_3[\text{MnMo}_6\text{O}_{18}((\text{OCH}_2)_3\text{CNH}_2)_2]$ (**1**) was prepared following the method given by Hasenkopf and co-workers,^[7b] though scaled down by a factor of ten and monitored over a longer period of time, that is, 30 h rather than 16 h: $((n\text{-C}_4\text{H}_9)_4\text{N})_4\text{-}[\alpha\text{-Mo}_8\text{O}_{26}]$ (0.80 g, 0.37 mmol), $\text{Mn}(\text{CH}_3\text{CO}_2)_3\cdot 2\text{H}_2\text{O}$ (0.15 g, 0.56 mmol), and $(\text{HOCH}_2)_3\text{CNH}_2$ (0.16 g, 0.13 mmol) were mixed in MeCN (15 mL; the stop clock started at this point). This mixture was stirred for 13 min at room temperature then the first 100 μL aliquot for MS testing was removed. The mixture was then set up to be heated at reflux at 80 °C with 100 μL aliquots removed for MS testing approximately every hour. (We started heating at reflux at 23 min on the stop clock.)

MS dilutions: Each 100 μL aliquot of reaction solution **1** was diluted to 10 mL with MeCN. Then 1 mL of this solution was made up to 5 mL with MeCN for direct injection into the ESI-MS system. All ESI-MS parameters were consistent throughout all data acquisitions. (See the Supporting Information for more detail on MS parameters and data acquisitions.) All MS data was collected using a Q-trap, time-of-flight MS (MicrOTOF-Q MS) instrument equipped with an electrospray ionization (ESI) source supplied by Bruker Daltonics

Ltd. The detector was a time-of-flight, microchannel plate detector and all data was processed using the Bruker Daltonics Data Analysis 4.0 software, whilst simulated isotope patterns were investigated using Bruker Isotope Pattern software and Molecular Weight Calculator 6.45.

Received: November 5, 2010

Published online: March 24, 2011

Keywords: manganese · mass spectrometry · polyoxometalates · self-assembly

- [1] a) P. Gouzerh, A. Proust, *Chem. Rev.* **1998**, *98*, 77; b) J. T. Rhule, C. L. Hill, D. A. Judd, *Chem. Rev.* **1998**, *98*, 327.
- [2] a) A. Müller, E. Beckmann, H. Bögge, M. Schmidtmann, A. Dress, *Angew. Chem.* **2002**, *114*, 1210; *Angew. Chem. Int. Ed.* **2002**, *41*, 1162; b) D.-L. Long, R. Tsunashima, L. Cronin, *Angew. Chem.* **2010**, *122*, 1780; *Angew. Chem. Int. Ed.* **2010**, *49*, 1736.
- [3] a) D. E. Katsoulis, *Chem. Rev.* **1998**, *98*, 359; b) T. Yamase, *Chem. Rev.* **1998**, *98*, 307; c) I. V. Kozhevnikov, *Chem. Rev.* **1998**, *98*, 171.
- [4] J. T. Rhule, W. A. Neiwert, K. I. Hardcastle, B. T. Do, C. L. Hill, *J. Am. Chem. Soc.* **2001**, *123*, 12101.
- [5] a) H. D. Zeng, G. R. Newkome, C. L. Hill, *Angew. Chem.* **2000**, *112*, 1841; *Angew. Chem. Int. Ed.* **2000**, *39*, 1771; b) C. Streb, C. Ritchie, D.-L. Long, P. Kögerler, L. Cronin, *Angew. Chem.* **2007**, *119*, 7723; *Angew. Chem. Int. Ed.* **2007**, *46*, 7579.
- [6] a) D.-L. Long, E. Burkholder, L. Cronin, *Chem. Soc. Rev.* **2007**, *36*, 105; b) H. N. Miras, G. J. T. Cooper, D.-L. Long, H. Bögge, A. Müller, C. Streb, L. Cronin, *Science* **2010**, *327*, 72; c) L. Xu, M. Lu, B. Xu, Y. Wei, Z. Peng, D. R. Powell, *Angew. Chem.* **2002**, *114*, 4303; *Angew. Chem. Int. Ed.* **2002**, *41*, 4129.
- [7] a) B. Hasenknopf, R. Delmont, P. Herson, P. Gouzerh, *Eur. J. Inorg. Chem.* **2002**, 1081; b) P. R. Marcoux, B. Hasenknopf, J. Vaissermann, P. Gouzerh, *Eur. J. Inorg. Chem.* **2003**, 2406.
- [8] a) Y. F. Song, H. Abbas, C. Ritchie, N. McMillian, D. L. Long, N. Gadegaard, L. Cronin, *J. Mater. Chem.* **2007**, *17*, 1903; b) Y. F. Song, D. L. Long, L. Cronin, *Angew. Chem.* **2007**, *119*, 3974; *Angew. Chem. Int. Ed.* **2007**, *46*, 3900; c) Y. F. Song, D. L. Long, S. E. Kelly, L. Cronin, *Inorg. Chem.* **2008**, *47*, 9137.
- [9] a) M. I. Khan, Q. Chen, J. Zubietta, D. P. Goshorn, *Inorg. Chem.* **1992**, *31*, 1556; b) Q. Chen, D. P. Goshorn, C. P. Scholes, X. L. Tan, J. Zubietta, *J. Am. Chem. Soc.* **1992**, *114*, 4667; c) A. Müller, J. Meyer, H. Bögge, A. Stammmer, A. Botar, *Z. Anorg. Allg. Chem.* **1995**, *621*, 1818.
- [10] a) Y. Q. Hou, C. L. Hill, *J. Am. Chem. Soc.* **1993**, *115*, 11823; b) C. P. Pradeep, D.-L. Long, G. N. Newton, Y.-F. Song, L. Cronin, *Angew. Chem.* **2008**, *120*, 4460; *Angew. Chem. Int. Ed.* **2008**, *47*, 4388.
- [11] A. J. Wilson, W. T. Robinson, C. J. Wilkins, *Acta Crystallogr. Sect. C* **1983**, *39*, 54.
- [12] a) L. Ma, S. C. Liu, J. Zubietta, *Inorg. Chem.* **1989**, *28*, 175; b) S. C. Liu, L. D. Ma, D. McGowt, J. Zubietta, *Polyhedron* **1990**, *9*, 1541; c) M. I. Khan, J. Zubietta, *J. Am. Chem. Soc.* **1992**, *114*, 10058.
- [13] A. Müller, J. Meyer, H. Bögge, A. Stammmer, A. Botar, *Chem. Eur. J.* **1998**, *4*, 1388.
- [14] a) H. N. Miras, D.-L. Long, P. Kögerler, L. Cronin, *Dalton Trans.* **2008**, 214; b) H. N. Miras, D. J. Stone, E. J. L. McInnes, R. G. Raptis, P. Baran, G. I. Chilas, M. P. Sigalas, T. A. Kabanos, L. Cronin, *Chem. Commun.* **2008**, 4703; c) H. N. Miras, J. Yan, D.-L. Long, L. Cronin, *Angew. Chem.* **2008**, *120*, 8548; *Angew. Chem. Int. Ed.* **2008**, *47*, 8420.
- [15] H. N. Miras, E. F. Wilson, L. Cronin, *Chem. Commun.* **2009**, 1297.
- [16] E. F. Wilson, H. Abbas, B. J. Duncombe, C. Streb, D.-L. Long, L. Cronin, *J. Am. Chem. Soc.* **2008**, *130*, 13876.
- [17] W. Henderson, J. S. McIndoe, *Mass Spectrometry of Inorganic and Organometallic Compounds*, Wiley, Chichester, **2005**.
- [18] Note that observation of reduced POM units at low mass could result from voltage effects (e.g. ion-transfer voltages and high collision energy voltage at low mass) utilized in the MS technique to investigate fragment ion species at low mass.
- [19] a) M. Bonchio, O. Bortolini, V. Conte, A. Sartorel, *Eur. J. Inorg. Chem.* **2003**, 699; b) D. K. Walanda, R. C. Burns, G. A. Lawrence, E. I. von Nagy-Felsobuki, *J. Chem. Soc. Dalton Trans.* **1999**, 311.
- [20] a) J. Gun, A. Modestov, O. Lev, D. Saurenx, M. A. Vorotyntsev, R. Poli, *Eur. J. Inorg. Chem.* **2003**, 482; b) F. Sahureka, R. C. Burns, E. I. von Nagy-Felsobuki, *Inorg. Chim. Acta* **2002**, 332, 7.
- [21] D. L. Long, C. Streb, Y. F. Song, S. Mitchell and L. Cronin, *J. Am. Chem. Soc.* **2008**, *130*, 1830–1832.
- [22] a) M. Filowitz, R. K. C. Ho, W. G. Klemperer, W. Shum, *Inorg. Chem.* **1979**, *18*, 93; b) V. W. Day, M. F. Fredrich, W. G. Klemperer, W. Shum, *J. Am. Chem. Soc.* **1977**, *99*, 6146.